A. R. Valente Pais*
Control and Simulation Division
Faculty of Aerospace Engineering
Delft University of Technology
Delft, The Netherlands

M. Wentink
TNO Defence, Security and Safety
Soesterberg, The Netherlands

M. M. van Paassen
M. Mulder
Control and Simulation Division
Faculty of Aerospace Engineering
Delft University of Technology
Delft, The Netherlands

Comparison of Three Motion Cueing Algorithms for Curve Driving in an Urban Environment

Abstract

Research on new automotive systems currently relies on car driving simulators, as they are a cheaper, faster, and safer alternative to tests on real tracks. However, there is increasing concern about the motion cues provided in the simulator and their influence on the validity of these studies. Especially for curve driving, providing large sustained acceleration is difficult in the limited motion space of simulators. Recently built simulators, such as Desdemona, offer a large motion space showing great potential as automotive simulators. The goal of this research is: first, to develop a motion drive algorithm for urban curve driving in the Desdemona simulator; and second, to evaluate the solution through a simulator driving experiment. The developed algorithm, the one-to-one yaw algorithm, is compared to a classical washout algorithm (adapted to the Desdemona motion space) and a control condition where only road rumble is provided. Results show that regarding lateral motion, the absence of cues in the rumble condition is preferred over the presence of false cues in the classical algorithm. "No motion" seems to be favored over "bad motion." In terms of longitudinal motion, the one-to-one yaw and the classical algorithm are voted better than the rumble condition, showing that the addition of motion cues is beneficial to the simulation of braking. In a general way, the one-to-one yaw algorithm is classified better than the other two algorithms.

1 Introduction

Over the years, research on car driving has been carried out with a multitude of purposes, as, for example, understanding and modeling the human driver behavior (Ritchie, McCoy, & Welde, 1968; Godthelp, Milgram, & Blaauw, 1984; Godthelp, 1986; Van Winsum & Godthelp, 1996), assessing potential dangerous driving situations, and studying drivers' reactions to driver assistance systems (Jamson, Whiffin, & Burchill, 2007) or new road designs. The advent of car simulators has improved time and cost-effectiveness, while allowing better control and repeatability of the experimental conditions. Furthermore, simulators offer a myriad of possible scenarios while guaranteeing the driver's safety. However, new possibilities bring new questions. The motion and visual stimuli presented to the subject in the simulator are not a replica of a real car situation. Especially regarding motion, many compromises

Presence, *Vol. 18, No. 3, June 2009,* 200–221

*Correspondence to a.r.valentepais@tudelft.nl.

have to be made to be able to maintain the simulator within its physical limits and still provide the driver with the necessary motion cues.

Research has been undertaken to investigate the effect of simulator motion on driving tasks (Repa, Leucht, & Wierwille, 1982; Siegler, Reymond, Kemeny, & Berthoz, 2001; Greenberg, Artz, & Cathey, 2003). Others have compared driver motion perception, behavior, and performance in a real car and in a simulator (Boer, Yamamura, Kuge, & Girshick, 2000; Panerai et al., 2001; Reymond, Kemeny, Droulez, & Berthoz, 2001; Siegler et al., 2001; Hoffman, Lee, Brown, & McGehee, 2002; Brünger-Koch, Briest, & Vollrath, 2006). In these studies, behavioral and performance metrics are used to assess the relative and absolute validity of the simulator (Blaauw, 1982). These measurements normally depend on the task at hand and no single metric can be used to summarize the driver's behavior. For braking maneuvers, measures related to the longitudinal control of the car are taken as, for example, maximum deceleration (Brünger-Koch et al.; Hoffman et al.; Siegler et al.; Boer et al.), mean jerk (Siegler et al.), vehicle speed (Brünger-Koch et al.; Panerai et al.), time to collision or time to the stop line when the subject initiates the braking maneuver (Boer et al.; Hoffman et al.; Brünger-Koch et al.). For lateral control maneuvers, such as lane change or cornering tasks, behavior and performance measures performed include the root mean square of the heading error and the lateral position error (Repa et al.; Greenberg et al.), the steering wheel angle and steering wheel reversal rate (Repa et al.), maximum lane position deviation (Repa et al.), mean trajectory (Siegler et al.), lateral acceleration (Reymond et al.), vehicle angular velocity (Siegler et al.) and curve approach speed (Boer et al.). The choice of objective metrics to be used in a simulator experiment is problematic, since it depends on the task difficulty and on predetermined performance goals. Furthermore, it is difficult to gather sets of studies that have used the same metrics to analyze the same issues. Consequently, the question of which motion cues are necessary for effective driving simulation is still an open one.

An especially challenging problem is cueing cornering tasks in urban environments. City curves have a smaller radius than highways or country roads. These sharp turns are thought to be more provocative than, for example, highway curves, and can cause disorientation or even motion sickness (Bertin, Collet, Espié, & Graf, 2005; Nilsson, 1993). Moreover, when a car enters a curve, there is an almost immediate onset of lateral acceleration due to the road curvature. Even at relatively low speeds, small curve radii can cause quite abrupt changes in lateral forces that are difficult to reproduce in a simulator. Both the quick onsets and the sustained forces throughout the curves play an important role in curve driving simulation (Greenberg et al., 2003; Kemeny & Panerai, 2003; Reymond et al., 2001; Siegler et al., 2001; Blaauw, 1982). Furthermore, not only is the curve radius small in urban environments, but also the curve angle is large. It is not uncommon to make 90° turns at a crossing or intersection with yaw rates of 30 deg/s (Grant, Papelis, Schwarz, & Clark, 2004). This type of scenario implies large yaw displacements that are difficult to render in simulators with a limited motion space. The concern about these problems is reflected in the recent development of driving simulators with a much larger motion space, as for example, a tilt platform (e.g., the hexapod) mounted on top of a rail or an XY table (Schwarz, Gates, & Papelis, 2003; Dagdelen, Reymond, Kemeny, Bordier, & Maïki, 2004; Jamson, Horrobin, & Auckland, 2007; Toyota News Release, 2007; Chapron & Colinot, 2007).

The Desdemona simulator, although it is structurally different from the ones described above, has a similarly large motion space. This makes it a quite attractive device to be used in road vehicle simulation. Moreover, the Desdemona central yaw axis can be used to simulate both the sustained lateral specific force as well as the yaw rate: the subject sitting in the cabin can actually drive through a curve (Valente Pais, Wentink, Mulder, & van Paassen, 2007).

The goal of the present research is twofold. The first part concerns designing and implementing a motion drive algorithm (MDA) for urban curve driving simulation in the Desdemona simulator. The new MDA makes use of the Desdemona centrifuge design to provide high angular rates and sustained accelerations. The second part consists of evaluating the new MDA through ex-

perimental comparison with two other motion algorithms. The evaluation of the three motion cueing algorithms will be done based on analysis of motion profiles, scores obtained from questionnaires, and objective measures of drivers' behavior and performance. However, since the task to be performed is relatively easy and no performance goals will be set, there is a limited number of objective metrics that can be used. Signals such as velocity, acceleration, and control inputs will be measured. From these, a variety of metrics can be calculated afterward. In the following sections, we will describe the Desdemona simulator and introduce the concept of motion cueing and motion filters. Then, the design of the new motion drive algorithm will be explained, as well as the other two MDAs that were used to create the three experimental motion conditions. Finally, we will describe the experimental method, present and discuss the results, and draw some conclusions.

1.1 The Desdemona Simulator

Figure 1 is a schematic of Desdemona with an indication of its 6 DOF. Table 1 summarizes the Desdemona motion space specifications. The simulator has an 8 m linear track. This linear track can rotate around its central point, providing a 4 m centrifuge arm. This DOF is denominated the "central yaw axis." Motion along the linear track represents displacement along the radius of the centrifuge, so this DOF is called the "radius" or "radius track." The structure mounted on the linear track consists of a 2 m vertical linear track, the "heave track." A gimballed structure mounted on the heave track allows the cabin to rotate more than 360° in three orthogonal axes. Using common aeronautical nomenclature, we name the rotations around the vertical axis "cabin yaw," around the lateral axis "cabin pitch," and around the longitudinal axis "cabin roll."

1.2 Motion Drive Algorithms

Compared to the real vehicle, all simulators have a restricted motion space. This means that a one-to-one replica of the vehicle motion is impossible to accomplish. Therefore, mathematical algorithms are used to transform real vehicle motion into simulator motion. These motion drive algorithms (MDAs), or motion filters, serve two purposes. The first is to maintain the simulator within its physical limits, observing not only the maximum displacement, but also velocity and acceleration constraints. The second is to provide the subject in the simulator with sufficient motion cues.

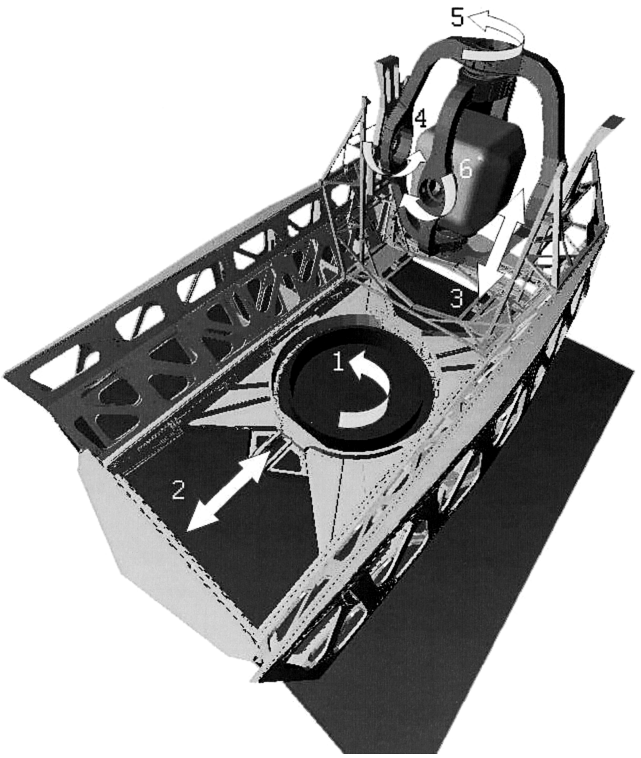

Figure 1. *Artistic impression of the Desdemona simulator with indication of the degrees of freedom: (1) central yaw axis, (2) radius track, (3) heave track, (4) cabin roll, (5) cabin yaw, and (6) cabin pitch.*

A widely known MDA is the classical washout algorithm (Reid & Nahon, 1985, 1986a, 1986b). This algorithm is mostly used in simulators using Stewart platforms, also known as hexapods. The methods used in this algorithm are common to other MDAs and will be briefly explained here as an introduction to motion cueing techniques. For the sake of clarity, we define here some terms used later in the paper. Linear accelerations refer to inertial linear accelerations excluding the gravity component. The combination of both linear acceleration and gravity is called specific force. Linear motion in

Table 1. *The Desdemona Simulator Motion Space Limits*

	Central yaw axis	Radius track	Heave track	Cabin roll	Cabin yaw	Cabin pitch
Position	>360°	±4.0 m	±1.0 m	>360°	>360°	>360°
Velocity	155 deg/s	3.2 m/s	2.2 m/s	180 deg/s	180 deg/s	180 deg/s
Acceleration	45 deg/s^2	4.9 m/s^2	4.9 m/s^2	90 deg/s^2	90 deg/s^2	90 deg/s^2

the vehicle or subject longitudinal, lateral, and vertical axes, are also referred to as surge, sway, and heave, respectively. Rotational movement around the longitudinal, lateral, and vertical axes are denominated roll, pitch, and yaw, respectively.

MDAs are a set of motion filters that transform vehicle motion into simulator motion. In the classical washout algorithm, sustained linear and angular accelerations are high pass filtered, so as the real vehicle accelerates, the simulator moves in the required direction to render the accelerations (onset cue). In order to prevent the actuators from reaching their limits while the real vehicle continues to accelerate, after the onset cue the simulator moves back to its initial position (washout). The washout creates a simulator motion opposite to the one in the real vehicle. This should optimally be done below the motion perception threshold of the subject. If the washout motion is above the perception threshold, then the return motion will be felt by the subject as a false cue. In driving simulation, sway motion can be used to provide the subject with the high frequency component of the lateral force present during a curve. When a car enters the curve, there is a quick onset of lateral force due to the road curvature. At this point, there will be a fast sway movement, followed by a slow washout motion that brings the simulator back to the initial position. When the car leaves the curve, there is a sudden decrease in lateral force. This means the simulator will sway in the opposite direction and again wash out to the initial position. Both sway motions, the onset-washout when entering the curve and the onset-washout when exiting the curve, are defined by the same high-pass filter, although only the first onset cue is desired. The filter settings should be such that the onset is strong enough to simulate entering the curve but not so strong that it causes a disturbing cue when leaving the curve. Furthermore, the washout motion should be kept below the perception threshold.

In addition to high-pass filtering, a technique called tilt coordination is also applied. The linear accelerations of the real vehicle are low-pass filtered and coupled to the angular channels. This means that as the real car accelerates forward, for example, the simulator cabin will slowly pitch up. If the tilting of the cabin is done below the rotation perception threshold, then the subject in the simulator will attribute the extra force in its longitudinal axis to a linear forward acceleration. This effect is stronger in the presence of visual cues. The combination of the onset cue from the high-pass filter and the tilting of the cabin tries to match the total linear acceleration of the vehicle. It exploits the fact that human sensors cannot distinguish between linear accelerations and gravity (Berthoz & Droulez, 1982). If there is no perception of angular motion, then an increase in specific force can be perceived as an increase in linear acceleration, instead of a different orientation relative to gravity (Groen & Bles, 2004).

This technique can be used in curve driving simulation to provide sustained lateral force using roll tilt. The amplitude of the provided lateral force will depend on the maximum roll angle. The larger the intended lateral force, the larger the maximum roll angle should be. To maintain a subthreshold roll rate, the cabin has to rotate slowly, causing the lateral force to build up gradually. This low frequency movement complements the quick onset cue provided by the fast sway movement. However, if the cabin takes too long to reach the desired roll angle, there will be a moment when the lateral force provided by the onset cue has passed and the one provided by the roll tilt is not present yet. This may cause a

drop in the perceived lateral force. Moreover, when the car leaves the curve, the sustained lateral force decreases abruptly. At this point, the cabin has to quickly rotate back. Again, to maintain the rotation below threshold, it will take some time before the cabin roll washout is finished. This can cause a lateral force false cue at the end of the curve. Thus, the choice of the cabin tilt rate limit is a compromise between, on the one hand, a quick buildup of the lateral force, a large enough maximum roll angle, and a fast roll washout, and, on the other hand, a roll rate that is below the perception threshold.

The classical washout algorithm, primarily designed for flight simulation in a hexapod, does not make optimal use of the Desdemona motion space. Hexapods can be referred to as parallel simulators (Angeles, 2003, pp. 6–10). The design of the motion cueing algorithms for parallel simulators might be considered independent of the motion platform. Although the tuning of the filters must account for the specific limitations and motion space of the platform, the filters' output is mostly expressed in translational and angular motion in an inertial frame of reference and not in the specific degrees of freedom of the simulator. Conversely, Desdemona may be considered a serial simulator, since each DOF is connected to the next, forming an open-loop kinematic structure. In Desdemona, the motion cueing strategy is closely related to the design of the simulator and its separate degrees of freedom. A general motion cueing strategy for Desdemona has been designed before, the spherical washout algorithm (Wentink, Bles, Hosman, & Mayrhofer, 2005). Although this filter makes better use of Desdemona's motion space than the classical washout algorithm, it is difficult to tune. We believe that an MDA specifically designed for Desdemona, with a defined task in sight, can make a much more effective use of the Desdemona motion space and motion characteristics.

2 Three Motion Filters

Three motion drive algorithms (MDAs) were implemented in the Desdemona simulator: the Rumble filter, the classical filter, and the one-to-one yaw filter. The rumble filter consisted of only road rumble motion. The classical filter was a classical washout algorithm, similar to the one described in Section 1.2, adapted to Desdemona's motion space. The one-to-one yaw filter was especially designed for curve driving in Desdemona, and as the name indicates, it provided a one-to-one yaw rate, with no need to wash out the lateral position.

2.1 The Rumble Algorithm

The first filter was designed to provide a control "no motion" condition. However, not moving the simulator at all would allow subjects to recognize this condition too easily, probably biasing the results. Therefore, the no motion condition was changed into a rumble only condition, that is, no car accelerations were cued but there was motion in heave and roll that mimicked the vibrations and oscillations due to the car engine and the road irregularities. The road rumble algorithm was developed at TNO, Soesterberg, and had been in use in TNO's small hexapod simulator. This motion condition provided the subjects with roll and heave motion with frequencies and amplitudes varying with car longitudinal velocity, but unrelated to the accelerations of the simulated vehicle (see Figure 2).

2.2 The Classical Algorithm

The second motion filter was a classical washout algorithm adapted to the Desdemona simulator motion space. The cabin initial or neutral position was halfway along the heave track and at 1 m from the end of the radius track. The cabin was oriented perpendicular to the radius track. Figure 3a shows the motion of the cabin in the horizontal plane when the simulated car makes a left turn. As the simulated car approached the turn (1) and braked (2), the cabin moved backward. The rotation of the central yaw axis was used to provide onset longitudinal acceleration. Small displacements in the radius and cabin yaw were used to maintain the specific force in the driver's longitudinal axis, as the central yaw axis rotated. When the car entered the curve (3) the cabin moved along the radius and the yaw gimbal

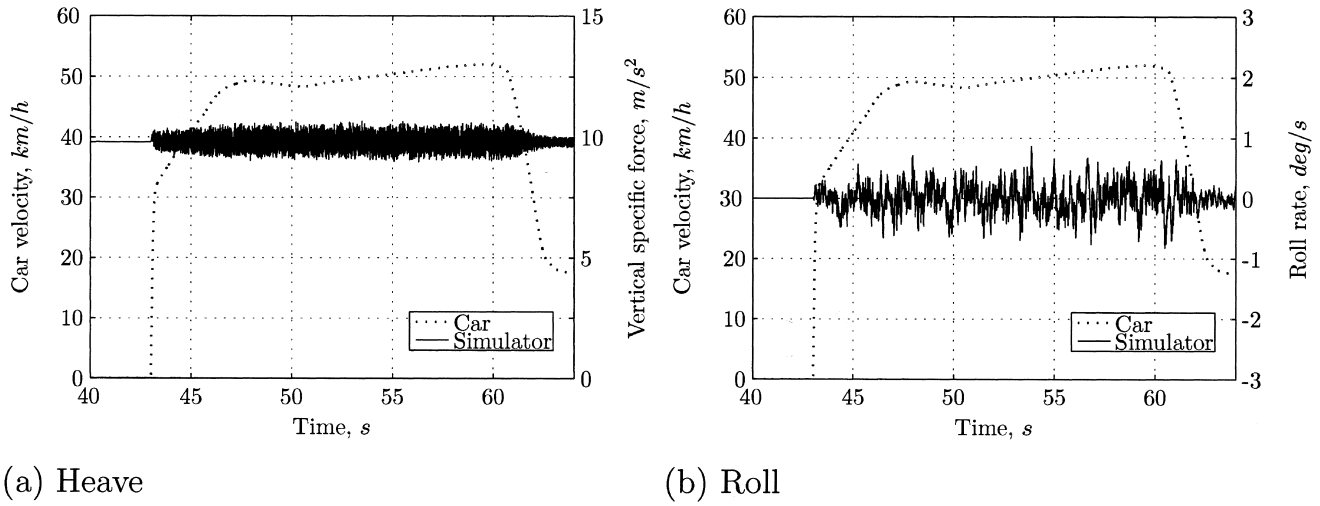

Figure 2. *Heave and roll simulator motion (solid line) varying with the car model longitudinal velocity (dotted line).*

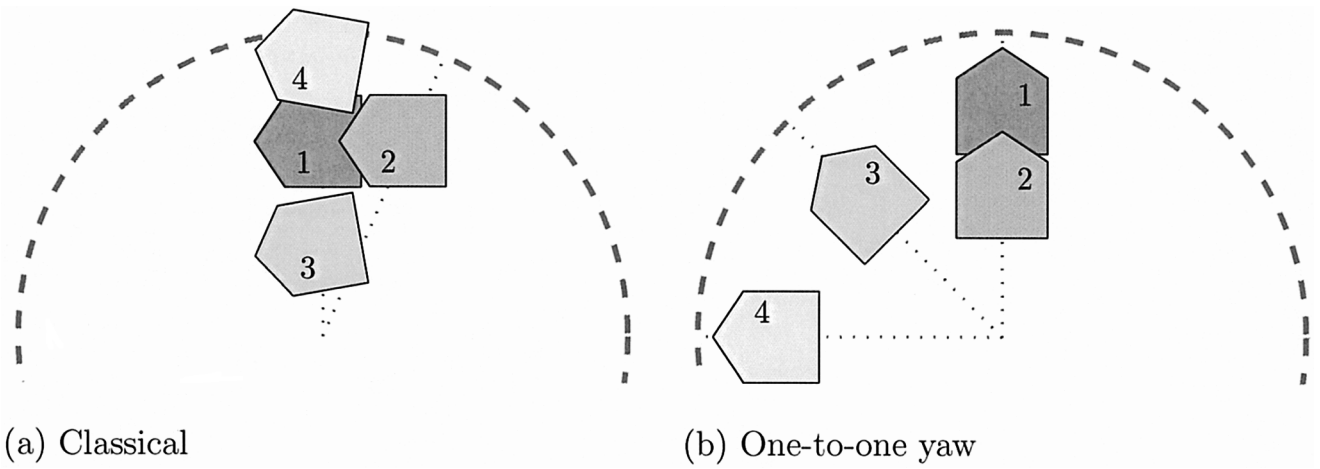

Figure 3. *Schematic of the cabin motion during one simulated left turn with the classical and the one-to-one yaw motion filter. Cabin position as the simulated car approaches the turn (1), brakes (2), turns left into the curve (3), and leaves the curve (4).*

turned, providing onset yaw and lateral acceleration. Coming out of the curve (4) generated a similar response as entering the curve, but with the cabin yaw and the displacement along the radius in the opposite direction. Between each movement, the cabin was washed out back to the neutral position. Cabin pitch and cabin roll were used throughout the experiment for tilt coordination and for onset cues in roll and pitch. The road rumble was simulated using the same algorithm as in the rumble filter.

2.3 The One-to-One Yaw Algorithm

The neutral position of the cabin was at 1.25 m from the end of the radius track and halfway along the heave structure. It was oriented radially, that is the cabin's longitudinal axis was parallel to the radius track, with the subjects facing outward. The two outer rings were in the horizontal plane, causing a gimbal lock. However, the impossible rotation was yaw, which could be done using the central yaw axis. The cabin could still

roll, using the yaw gimbal, and pitch, using either the pitch or the yaw gimbals. Figure 3b shows the position of the cabin throughout a simulated left turn. When the simulated vehicle approached the turn (1), it decelerated (2). The cabin moved backward along the radius track providing the subject with onset longitudinal acceleration cues. When the vehicle entered the curve (3), the central yaw axis rotated at the same yaw rate as the car. The tangential acceleration from the rotation of the yaw axis, and not the centripetal acceleration, as one would expect, was used to simulate the lateral forces. When the car left the curve (4), the yaw axis decelerated. Since the central yaw axis did not have limited displacement, there was no need to bring it to the neutral position, so there was no lateral position or yaw angle washout. Pitch motion was used to provide sustained longitudinal specific forces and to compensate for the centripetal acceleration generated by the rotation of the central yaw axis. Roll motion was also used to provide sustained lateral specific forces. For the road rumble, we used the same algorithm as in the rumble filter.

Figure 4 shows a block diagram of the developed motion cueing algorithm. The main elements will be analyzed in more detail in the following sections.

2.3.1 Longitudinal and Vertical Motion. In Figure 4, HP_{radius} and HP_{heave} were composed of a first order high-pass filter $HP_{1\text{st}}$ followed by a second order high-pass limiting filter ($HP_{2\text{nd lim}}$). The specific forces at the driver's head (f_{car}) were transformed to the subject's longitudinal and vertical axis, using the cabin orientation (Θ). The calculated x and z components of the specific force were then filtered and coupled to the radius and heave DOFs, respectively. The output of the filters HP_{radius} and HP_{heave} were the commanded motion of the radius and heave DOFs in terms of position, velocity, and acceleration. The limiting filter ($HP_{2\text{nd lim}}$) had two working modes: high-pass filter mode or limiting mode. After high-pass filtering the signal, the limiting algorithm looked at the current position, velocity, and acceleration to predict the position in the near future. Depending on the calculated future position, one of the two working modes was chosen. If the future position was within the position limits, no limiting was necessary. This meant that the output of the total limiting filter ($HP_{2\text{nd lim}}$) was simply the input signal after a second order high-pass filter (cueing motion). On the other hand, if the future position exceeded the position limits, the limiting mode took over by braking the simulator and repositioning it at a safe distance (limiting motion). The simulator maximum velocity and acceleration were limited for both working modes, so both the cueing motion as well as the limiting motion had limited velocities and accelerations, although different limits were used for the two modes. The first order filter, $HP_{1\text{st}}$, prevented the limiting filter, $HP_{2\text{nd lim}}$, from alternating between the two modes continuously, when the input was a high sustained acceleration signal. This would cause the simulator to oscillate between the safe distance and the position limit.

2.3.2 Lateral Motion. The central yaw axis was used to provide both the lateral specific forces and the yaw rotation. The car yaw velocity (ω_z) was coupled almost directly to the central yaw axis rotational velocity. In Figure 4, $LP_{1\text{st lim}}$ was a low-pass filter with velocity and acceleration limiting. However, the cutoff frequency was sufficiently high that the filter approximated unity at the frequencies of interest, resulting in a one-to-one yaw rate. The output of this filter was the motion of the central yaw axis in terms of position, velocity, and acceleration. The tangential acceleration generated by the acceleration and deceleration of the central yaw axis simulated the lateral forces through the curve. However, the accelerations generated were not large enough, so to increase the lateral specific forces during the curves, the cabin was tilted in roll. Increasing the rotational acceleration of the central yaw axis could provide higher tangential accelerations, thus decreasing or even omitting the roll rotation. However, this would also increase the resultant centripetal acceleration. Accordingly, there would be higher specific forces in the subjects' longitudinal axis that would require faster pitch rotation. Thus, the choice of the central yaw axis rotational acceleration was actually a compromise between adding some roll rotation or increasing the pitch rotational acceleration to eventually supra-threshold levels.

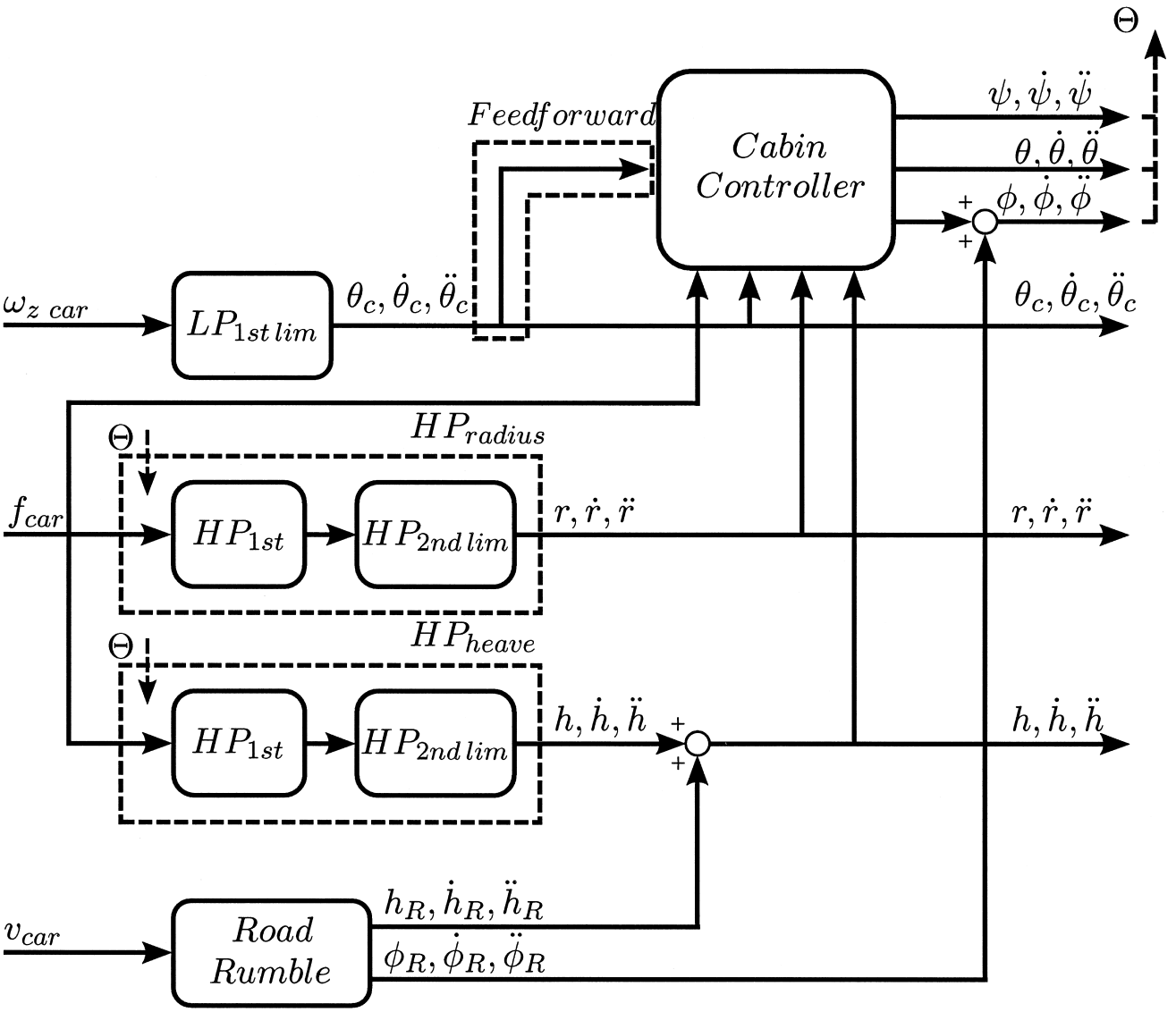

Figure 4. *Block diagram of the one-to-one yaw motion cueing algorithm.*

2.3.3 Tilt Coordination and the Cabin Controller. In addition to roll, pitch rotation was also used to provide sustained specific forces. Pitch tilt complemented the radius track onset cues and compensated for the centripetal force associated with the central yaw axis rotation. The tilt coordination algorithm was implemented in the block *Cabin Controller* in Figure 4. The inputs for the *Cabin Controller* were the motion of the first three DOFs of the simulator (central yaw axis, radius, and heave) and the desired specific forces at the subject's head (f_{car}). From the inputs, the specific forces generated by the motion of the first three DOFs (f_3) were computed. Then, the *Cabin Controller,* using only the pitch and roll DOFs, oriented the cabin so that the direction of f_3 coincided with the direction of f_{car}. To improve the timing of the cabin roll rotations with the desired lateral forces, we fed forward the car yaw rate (ω_z) to the roll channel of the *Cabin Controller*. The car

yaw rate signal was used, instead of the lateral specific force signal, for two reasons. First, in the type of curves we used, the shape of the two signals was generally the same. Second, the car yaw rate signal was much smoother than the lateral specific force signal.

3 The Experiment

3.1 Hypotheses

From the three implemented motion filters, we expected the one-to-one yaw filter to be rated best by subjects. The one-to-one yaw filter provided more motion than the rumble filter, which we expected to be favorable to the realism of the simulation. Compared to the classical algorithm, the one-to-one yaw filter did not need to wash out either lateral position or yaw angle and provided a one-to-one yaw, instead of only yaw onset cues. We hypothesized that these features would improve the realism of lateral motion during turns.

With respect to motion sickness, we expected the classical filter to be the most provocative due to the existence of false cues during the washout of the roll angle. The rumble filter, since it provides very little motion, was hypothesized to be the least provocative. We also expected that if subjects did get motion sick, then throughout the experiment that condition would worsen, that is, motion sickness would tend to increase throughout the experiment.

3.2 Method

3.2.1 Apparatus. The experiment was performed in the Desdemona simulator. The cabin was equipped with a generic car cockpit, as shown in Figure 5.

The visual database was built using StRoadDesign (STSoftware, 2008) and OpenSceneGraph (Burns & Osfield, 2004). A PC-based computer generated image system was used to render the outside world. In the cabin, three computers generated real-time images with an update rate of 60 Hz. Three projectors (resolution: 1024×768 pixels) projected the image on a three part flat screen, placed at approximately 1.5 m from the driver's eyes, creating an out-of-the-window field-of-view of 120° horizontal and 32° vertical. Blending and image distortion was also computed in the three computers in the cabin.

Figure 5. *The interior of the Desdemona cabin with the car cockpit installed. Outside world view from the driver's perspective.*

The dashboard consisted of a speedometer displayed on an LCD screen, placed behind the steering wheel and connected to the on board I/O computer. The sound system was developed at TNO. It reproduced wind and engine sound depending on vehicle velocity and engine. Direct drive electrical motors placed inside the cabin provided the control loading for the steering wheel, the gas, and the brake pedals. Pedals and steering wheel position and velocity were read by the on board I/O computer with a sampling frequency of 1 MHz for the pedals and 100 Hz for the steering wheel. The I/O computer connected the controls, the dashboard, and the audio system to the vehicle model at a frequency of 400 Hz.

On the "shore," two computers ran the car model and the motion filters. The car model was implemented as an *s*-function generated by CarSim, running on MATLAB Simulink at 400 Hz. The motion filters were also implemented in MATLAB Simulink and ran at a frequency of 200 Hz. One supervisor computer hosted the operator interface and logged data. The commanded motion was sent from the motion filters to the Desdemona computer via a bridge computer with a frequency of 200 Hz.

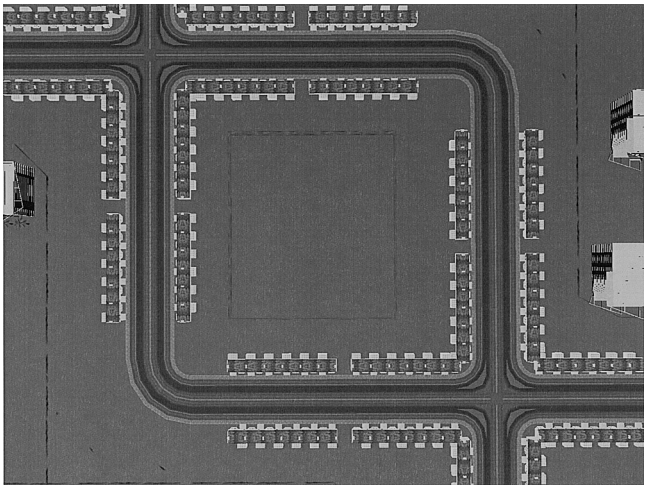

Figure 6. *Top view of the driving circuit: a square city block with 150 m straight segments, two 20 m radius curves, and two intersections.*

3.2.2 Experimental Design and Procedure. An experiment was performed using three different motion filters: the rumble, the classical, and the one-to-one yaw filters, described in Section 2. Using each motion filter, subjects drove two times around a square city block, performing only left turns. Figure 6 shows the top view of the circuit. Two of the turns were 20 m radius curves and the other two, in diagonally opposite corners, were perpendicular crossings, or intersections, with rounded shoulders. The radius of the rounded shoulders was 8.5 m.

After each run (eight left turns), the subjects answered a questionnaire. After the first and last run they also filled in a motion sickness scale. At the end of the experiment they were asked to rank the three filters according to their preference. Each subject performed four runs: three experimental runs and one trial run. The trial run was performed with the same motion filter as the first experimental run. The presentation order of the motion filters was randomized and balanced for all subjects. Between each run there was time for the subjects to fill in the questionnaire and the motion sickness scale. Subjects indicated when they were ready for the next run. The total time inside the simulator, per subject, was between 20 and 30 min.

3.2.3 Questionnaires and Motion Sickness Scale. The questionnaires consisted of seven questions to be answered by placing a mark on an analog scale, one mark per scale. The analog scales were represented by a horizontal line of 10 cm with beginning, middle, and end markings. The extremes of the scale were from totally unrealistic motion, on the left, to just like a real car, on the right. Subjects were asked to answer the following questions:

1. How realistic or unrealistic was the overall motion while driving, specially focusing on the curved segments (curves and intersections)?
2. How easy or difficult was it to steer the car (staying on the lane)?
3. How realistic or unrealistic did the road rumble feel?
4. How realistic or unrealistic did entering the curves feel?
5. How realistic or unrealistic did leaving the curves feel?
6. How realistic or unrealistic did accelerating feel?
7. How realistic or unrealistic did braking feel?

There are several motion sickness scales available (Kennedy, Lilienthal, Berbaum, Baltzley, & McCauley, 1989; Kennedy, Lane, Berbaum, & Lilienthal, 1993). The motion sickness scale used was the misery scale (MISC), developed and validated at TNO Human Factors (Wertheim, Ooms, de Regt, & Wientjes, 1992), as shown in Table 2.

3.2.4 Subjects and Subjects' Instructions. Twenty-four volunteer subjects participated in the experiment. Subjects were aged from 23 to 58 (the mean was 33 years, the median was 31 years), with a driving experience between 2 and 39 years (the mean was 13 years, the median was 12 years). All but two subjects had experience with automatic gearshift cars. All but six subjects had had previous experience with some sort of vehicle simulator.

Subjects did not see the simulator move in any of the motion conditions before they went in for the experiment. We instructed subjects to drive like they normally would in their cars, trying to keep the car in the center

Table 2. *The MISC: The Rating Scale Used to Evaluate Motion Sickness*

Symptom		Score
No problems		0
Slight discomfort but no specific symptoms		1
Dizziness, warm, headache, stomach awareness, sweating, and so on	Vague	2
	Some	3
	Medium	4
	Severe	5
Nausea	Some	6
	Medium	7
	Severe	8
	Retching	9
Vomiting		10

of the right lane and keeping an acceptable velocity. They were reminded that it was a city environment and the speed limit was 50 km/hr (31 mi/hr). With respect to the questionnaires, we asked subjects to consider the simulator motion to answer the questions, that is, not to focus too much on other simulation features like the visuals, the dashboard, or the lack of mirrors and car frame. Also, we advised them to take as a reference a rental car, a small family car with an automatic gearshift. By doing so, we tried to establish an absolute reference, common for all subjects.

4 Results

4.1 Simulator Motion

The three motion filters resulted in three different simulator motion profiles. For the rumble filter, the resulting motion was quite trivial and consisted of high frequency motion in roll and heave. For the classical and one-to-one yaw filters it is interesting to look at the motion space used by the two filters, as shown in Figure 7.

In terms of longitudinal motion, the motion space used was equivalent for both motion filters. The tuning of the longitudinal channel was quite conservative and that can be seen in the limited motion space used, approximately half a meter. The lateral cueing in the one-to-one yaw filters was done using the central yaw axis, which led to the 360° footprint shown in Figure 7b.

For the one-to-one yaw and classical filters, the motion provided to the subject in the simulator and in the car was compared. The specific forces and yaw rate at the subject's head for one subject during four curves are displayed in Figure 8. The car signals were computed from the output of the car model and the simulator signals from the output of the motion filters.

The longitudinal cueing of both algorithms have similar characteristics, so the differences in the resulting longitudinal specific forces are minimal.

With respect to the lateral specific forces, the one-to-one yaw filter provided higher magnitudes than the classical. Tuning the classical filter to provide higher amplitudes of lateral specific force would lead to higher roll angles that would also take longer to wash out, increasing the occurrence of situations like the one depicted in Figure 9. In this case, the washout of the roll angle in the classical filter was too slow, causing a peak in lateral force at the end of the curve. We relate this artifact to the many subjects' reports of feeling tilted sideways when coming out of the curve. The different behavior

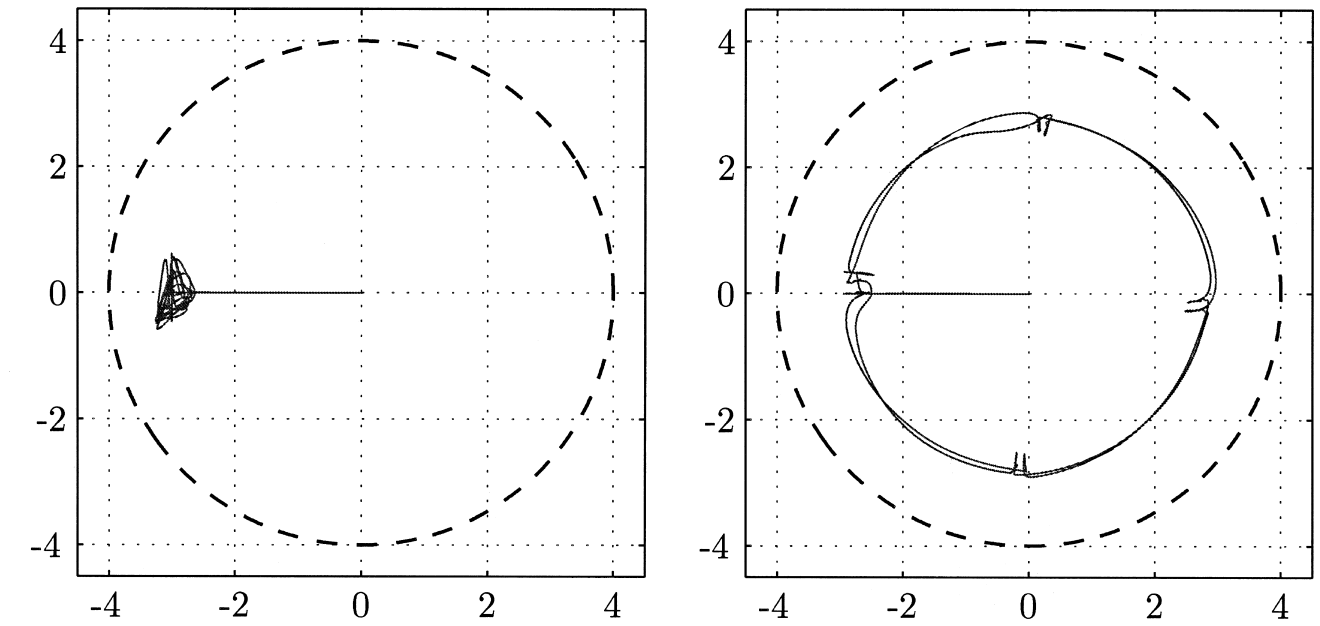

Figure 7. *Motion space used by the classical and the one-to-one yaw filters: footprint of the cabin motion (gray line) and simulator maximum radius (dashed black line).*

of the classical motion filter shown in Figure 9 was related to the subjects' driving strategies: a combination of chosen velocity and trajectory. The one-to-one yaw filter allowed roll rates of 6 deg/s in tilt coordination, twice as high as in the classical algorithm. Nevertheless, there were no complaints from subjects regarding false roll cues in the one-to-one yaw filter.

The major difference between the two motion filters, one-to-one yaw and classical, was the yaw motion (see Figure 8e and Figure 8f). In a real car, driving into a curve results in an initial angular acceleration in the direction of the curve (positive) and then, leaving the curve, there will be an angular acceleration in the opposite direction (negative). With the classical filter, only onset cues were provided. This means that the cabin first turned in the positive direction (onset) and then immediately returned to the initial orientation (washout). When leaving the curve, a similar behavior occurred: the cabin turned in the negative direction (onset) and then immediately returned to the initial orientation (washout). This behavior resulted in the yaw rate depicted in Figure 8e. The one-to-one yaw algorithm, on the other hand, did not have a washout, since the yaw cue was provided one-to-one using the central yaw axis.

4.2 Questionnaires: Drivers' Ratings

The answers to the questionnaires were converted from the analog scale to a numerical value from 0 to 10. This numerical value was taken as the score on each of the seven questions in the questionnaire. The means of the scores, adjusted for all subjects (Field, 2005, pp. 279–285) and the 95% confidence interval of the means are shown in Figure 10a and in Figure 11. Each plot corresponds to a question on the questionnaire: overall score, ease of driving, road feel, entering the curves, leaving the curves, accelerating, and braking.

Figure 10 shows that with respect to the overall realism of the motion, the one-to-one yaw filter scored

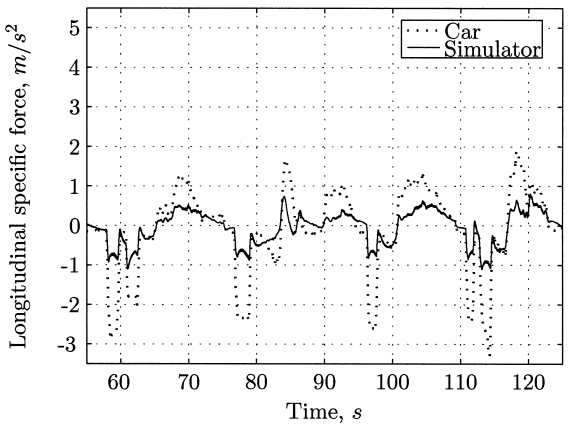

(a) Classical

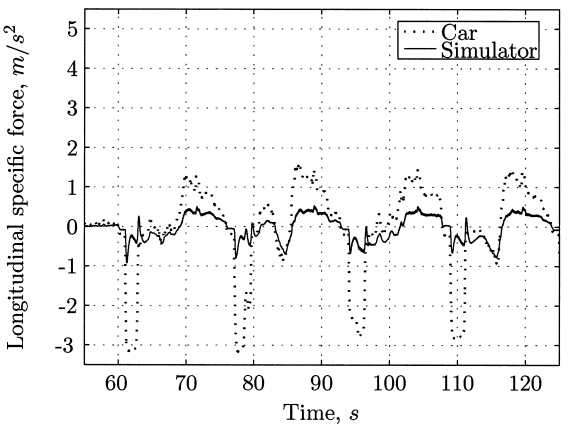

(b) One-to-one yaw

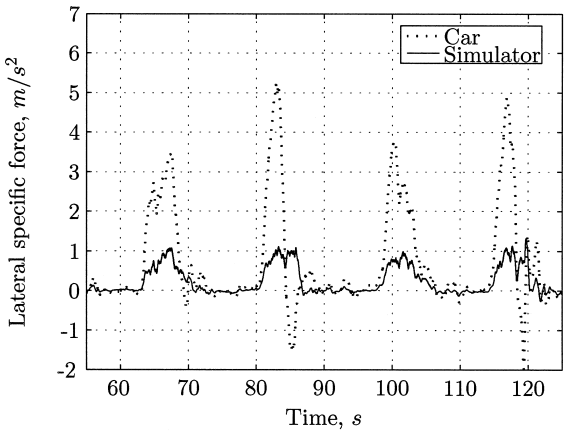

(c) Classical

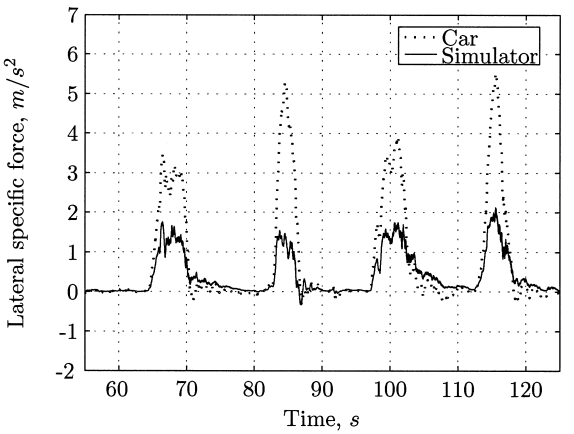

(d) One-to-one yaw

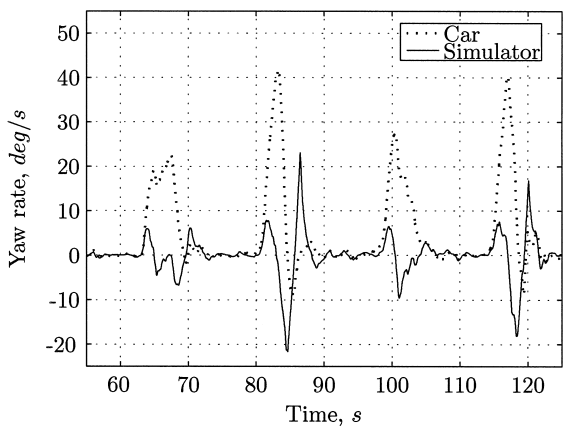

(e) Classical

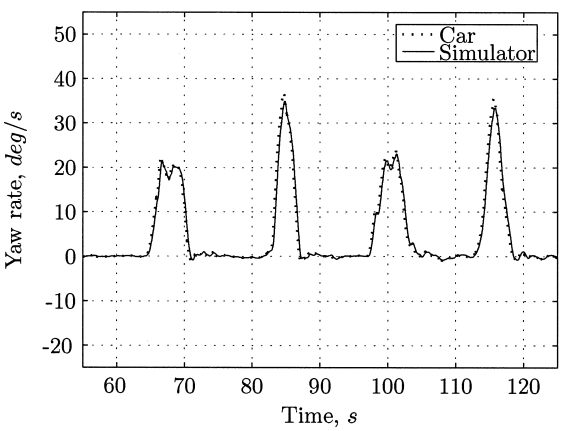

(f) One-to-one yaw

Figure 8. *Longitudinal and lateral specific forces and yaw rate at the subject's head from the car model and in the simulator with the classical and one-to-one yaw motion filters during four curves.*

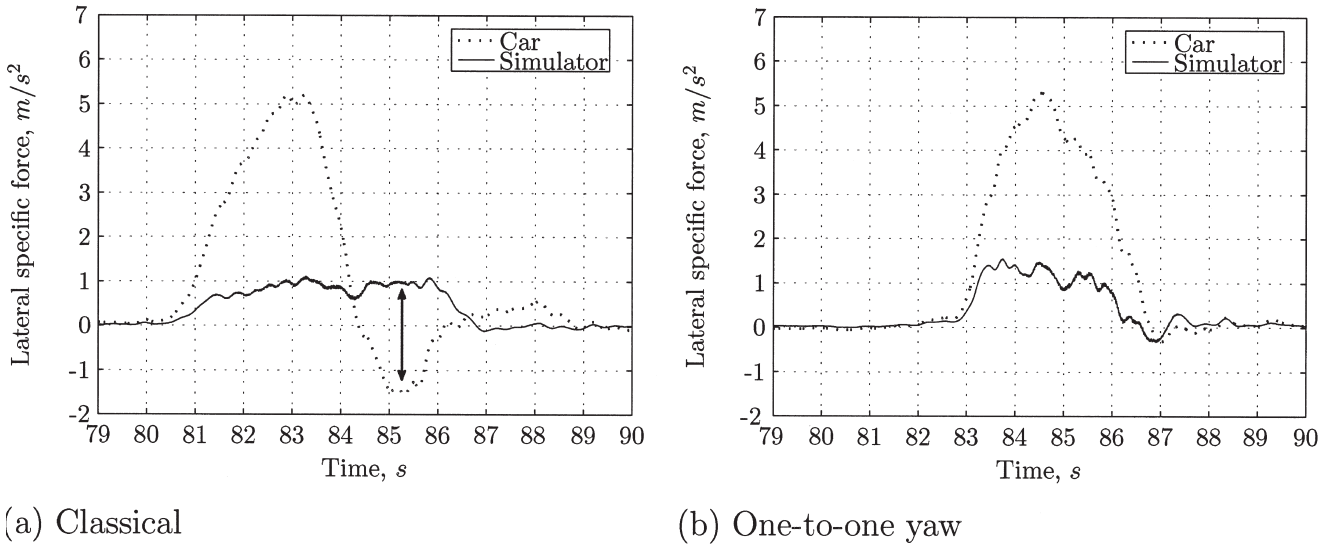

Figure 9. *Lateral specific force at the subject's head from the car model and in the simulator for one subject driving the same curve with two different motion conditions: the classical and the one-to-one yaw motion filters. At the end of the curve, the slow washout of the roll angle with the classical algorithm causes a false cue in lateral force.*

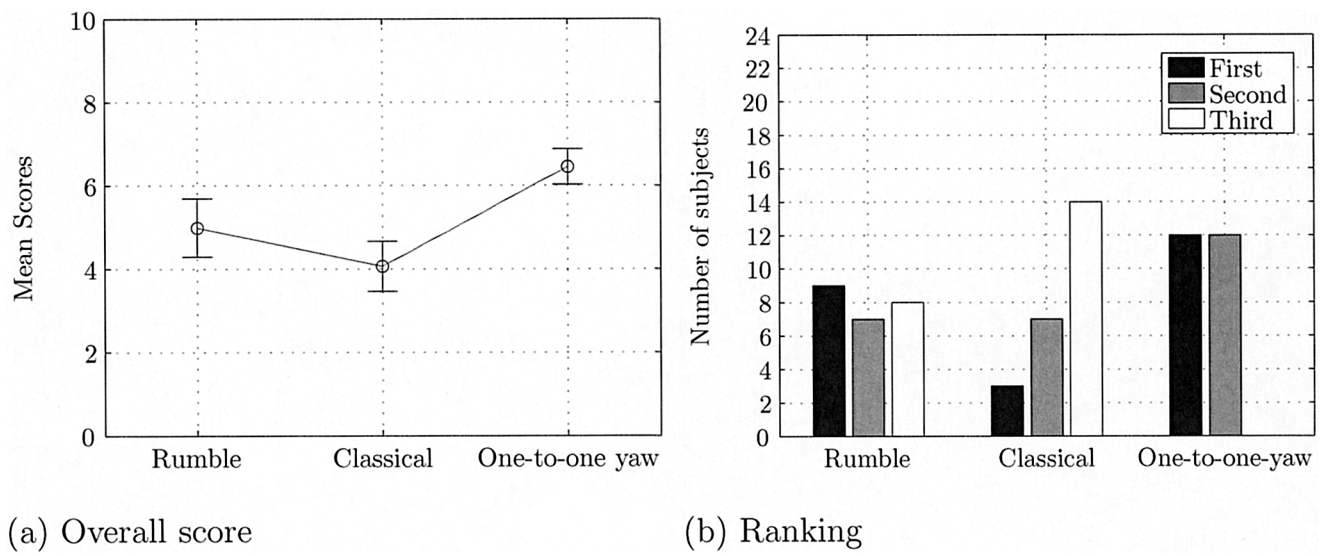

Figure 10. *Realism of the simulator motion for the three motion conditions from the scores on the questionnaire and the results of the ranking question. The bars in (a) represent the 95% confidence interval of the means.*

best, rumble second, and classical last. The results of the ranking question are shown in Figure 10b. The one-to-one yaw filter was voted as the best by half of the subjects and the other half placed it in second place. The classical filter was classified third by more than half the subjects and the rumble filter was classified first, second and third almost the same number of times.

A repeated measures ANOVA was performed on the

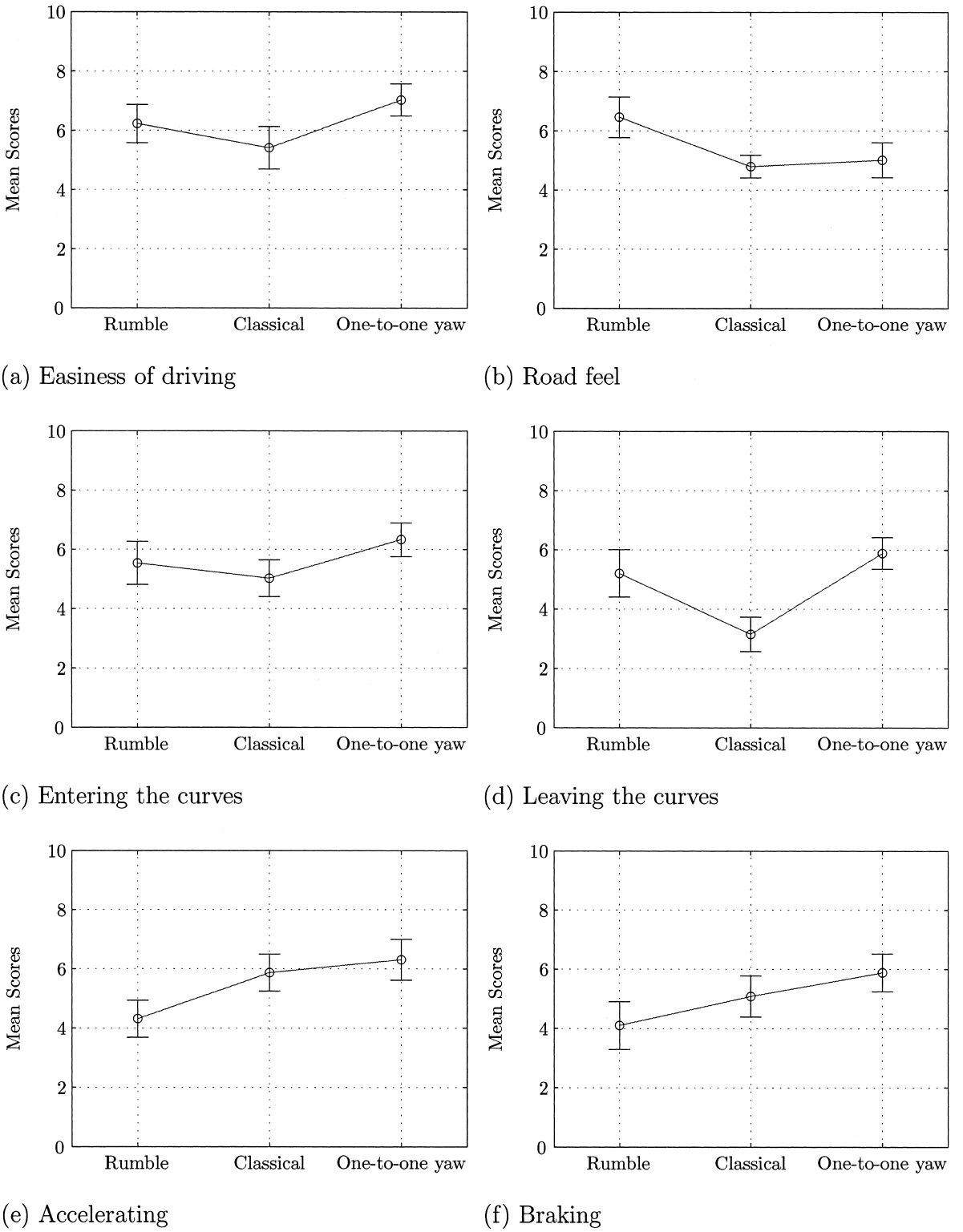

Figure 11. *Answers to the questionnaire. Mean scores and the 95% confidence interval of the means (from 0, not realistic at all, to 10, just like a real car).*

Table 3. *ANOVA and Post Hoc Test Results of the Answers to the Questionnaire*

	ANOVA			Pairwise comparison		
Question	DOF	*F*	Sig.	R-C	R-O	C-O
Total score	(1.58, 36.30)	12.08	**	—	*	**
Ease of driving	(2, 46)	4.55	*	—	—	*
Road feel	(1.45, 33.45)	7.77	**	**	—	—
Entering curves	(2, 46)	2.80	—	*n.a.*	*n.a.*	*n.a.*
Leaving curves	(1.56, 35.96)	13.65	**	*	—	**
Accelerating	(2, 46)	7.49	**	*	**	—
Braking	(2, 46)	4.42	*	—	*	—

*: significant ($p < 0.05$)
**: highly significant ($p < 0.01$)
—: not significant
n.a.: not applicable

scores on each question. The independent variable was the motion filter (rumble, R, classical, C, and one-to-one yaw, O) and the dependent measures were the scores on each of the questions in the questionnaire. There was a significant effect of the motion filter on the scores for all questions except question 4: realism of the motion entering curves. For all other questions, post hoc pairwise comparisons were performed using Bonferroni correction for the level of significance (Field, 2005, pp. 339–341). Table 3 shows the results of the ANOVA and the post hoc tests.

On the question about the overall realism, the one-to-one yaw filter had a significantly higher score than rumble and classical. Regarding the ease of driving, the one-to-one yaw filter also had the highest score, significantly higher than the classical but not significantly higher than the rumble filter. On question 3, the realism of the road feel, the rumble filter scored best, significantly higher than the classical but not significantly higher than the one-to-one yaw filter.

Lateral motion was evaluated by questions 4 and 5. On question 4, the realism of the motion while entering curves, the one-to-one yaw filter scored best, rumble second, and classical last. Also, leaving the curves, the classical filter was considered the worst of the three. However, whereas the differences in scores while entering the curves are not statistically different, leaving the curves, the classical condition shows a significantly lower score.

Regarding longitudinal motion, accelerating was considered significantly more realistic in the conditions with motion than with the rumble condition. Similarly, braking with the one-to-one yaw condition was significantly better than the rumble condition but was not statistically different from the classical algorithm. However, for the braking maneuvers, there was no statistical difference between the classical and the rumble filters' scores.

4.3 Motion Sickness Scales

Out of all the subjects, only one left in the middle of the test due to motion sickness. We then asked one more subject to perform the experiment, to keep a balanced design. Twenty-four subjects finished the experiment, from which eight started with the rumble filter, eight with the classical filter, and eight with the one-to-one yaw filter. An independent one-way ANOVA was performed to evaluate the difference in motion sickness scores after the first run. To evaluate the scores on the MISC, the subjects who did not get sick at all (subjects

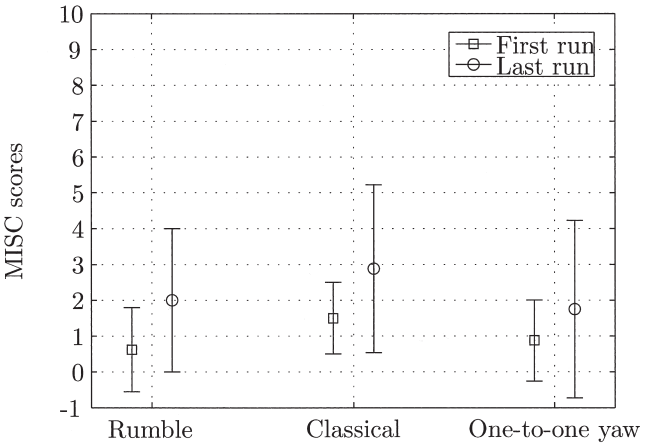

Figure 12. *Scores on the MISC. Mean and the 95% confidence interval of the mean of the MISC scores after the first and last run, for the motion filter presented first to the subjects.*

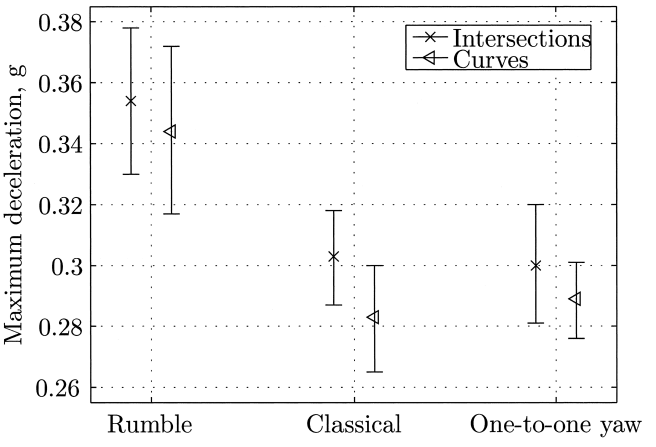

Figure 13. *Mean maximum deceleration for each motion filter and section of the trajectory. The error bars represent the 95% confidence interval of the means.*

who scored zero twice on the MISC) were excluded from the statistical analysis. In total, eight subjects were excluded from the data set: three had started with the rumble filter, two with the classical, and three with the one-to-one yaw filter. The subjects who started with the classical filter presented the highest scores on the MISC and the ones who started with the rumble filter presented the lowest scores. However, the ANOVA showed that the motion filter did not have a significant effect on the MISC scores, $F(2, 13) = 0.72$, $p > .05$.

The cumulative trait of motion sickness was evaluated by performing a repeated measures ANOVA to compare the MISC scores after the first run and at the end of the experiment. There was indeed a significant increase, $F(1, 15) = 11.52$, $p < .01$, from the scores after the first run ($M = 1.5$, $SE = 0.34$) to the scores at the end of the experiment ($M = 3.3$, $SE = 0.66$). Figure 12 shows the MISC scores after the first run and at the end of the experiment for the motion filter presented first to the subjects.

4.4 Objective Measures

We expected the subjects to adopt a different driving behavior or have a different performance depending on the motion filter. We measured different signals, such as steering wheel angle, brake and gas pedal deflection, lateral and longitudinal acceleration, and velocity. The only metric for which we found a relevant and statistically significant effect of the motion filter was on the maximum deceleration. The majority of times, subjects pressed the brake pedal at the final part of a straight segment and continued pressing it in the beginning of the curve or intersection. Thus, the two laps around the square city block were divided in two sections: the intersections including the straight segment before the intersection; and the 20 m radius curves also including the straight segment before the curve. For each filter, we computed the maximum deceleration in each of these sections. Each driver, in each motion condition, drove each section of the trajectory four times. For the statistical analysis, we used the average of the values calculated for the second and third runs. Figure 13 shows the average maximum deceleration in each section of the trajectory. The values displayed are the adjusted means for all subjects (Field, 2005, pp. 279–285), for each motion filter and section of the road.

The data were analyzed using a two-way, repeated measures ANOVA. The independent variables were the motion filter (rumble, classical, and one-to-one yaw) and the road section (intersection and curve). The dependent measure was the maximum deceleration.

Mauchly's tests indicated that the assumption of sphericity was violated for some of the effects. In these cases, we used Greenhouse-Geisser estimates of sphericity to correct the degrees of freedom. We also performed post hoc pairwise comparisons using Bonferroni correction for the level of significance (Field, 2005, pp. 339–341). The ANOVA showed a significant effect of the motion filter, $F(1.36, 31.27) = 9.996$, $p < .01$, and of the section of the trajectory, $F(1, 23) = 5.23$, $p < .05$, on the maximum deceleration. The post hoc tests indicated that the maximum deceleration was significantly lower ($p < .05$) with the classical ($M = 0.29$, $SE = 0.009$) and one-to-one yaw ($M = 0.30$, $SE = 0.009$) filters than with the rumble filter ($M = 0.35$, $SE = 0.014$).

5 Discussion

In the present study, experiments with three motion drive algorithms for car driving have been performed. This study did not include real car driving and even in the literature not much data from actual car experiments were found. Therefore, the motion drive algorithms are mainly compared against each other in terms of their use of motion space and with respect to the subjective ratings of driving realism and motion sickness. The maximum brake acceleration could be compared to values found in literature from both simulator and real car studies.

5.1 Simulator Motion

The longitudinal motion cueing of the one-to-one yaw filter was very similar to the classical washout. However, since this was the first experiment to run in the Desdemona simulator, extra care was taken for the motion constraints. To prevent the simulator from reaching the radius arm limits during any part of the experiment, the longitudinal motion tuning was very conservative. Less conservative filter parameters would allow better use of the motion space.

In the one-to-one yaw algorithm, the maximum roll rates were twice as high as the typical 3 deg/s used in tilt coordination, without complaints from the subjects. In our opinion, two things explain this result. First, the feed-forward loop provided a roll rate that was much better timed to the onset of lateral force. Second, in a real vehicle, there is a roll onset while entering and leaving a curve. The provided roll rate fit the expected vehicle roll, making it easier to be accepted as a good cue. We think this technique can be used in other types of vehicle simulation, such as flight simulation. The success of the tilt coordination using the feed-forward loop lies in the choice of driving signal. In this case, we used the vehicle yaw rate, which had the same shape as the desired roll angle.

5.2 Questionnaires: Drivers' Ratings

The one-to-one yaw filter scored best in terms of realism of the simulation. Both the scores on the question about the overall realism and the ranking results confirm that the order of preference was the one-to-one yaw filter first, second the rumble, and third the classical. The question about the ease of driving showed the same order of preference. The road feel was less realistic in the conditions with motion (classical and one-to-one yaw filters). Some subjects reported that the feel of the road in these conditions was too strong and it sometimes felt like they were driving a small truck. This result probably reflects an interaction between the road feel cueing and the vehicle motion cueing, which amplified the simulator accelerations.

Looking at the questions about lateral motion entering and leaving curves, the one-to-one yaw filter scored best and the classical worst. When leaving the curve with the classical filter, many subjects reported feeling tilted when coming out of the curve. Some of the subjects added that it was sickening, disorienting, or simply unpleasant. This led us to believe that the lower scores of the classical filter in this question were due to this artifact. With the rumble condition there were no lateral cues, except for roll vibrations, and still the score was just slightly lower than with the one-to-one yaw filter. More obvious differences on paper, such as the one-to-one yaw rate provided in the one-to-one yaw filter, were not positively noted by the subjects, not even in the ex-

perimental debriefing. These observations indicate that the scores reflect not so much good cueing as they do bad cueing or bad motion. The presence of false cues, even brief ones, are strongly penalized, whereas the absence of both good cues and false cues, as in the rumble condition, seem to be tolerated quite well.

Regarding the longitudinal motion, the one-to-one yaw filter scored best and the rumble condition worst. It seems that here, unlike in the lateral case, there was a recognition of the lack of good cues. The rumble filter was not reported to be disturbing or disorienting, but some subjects did report that something was missing, although others also said that the acceleration and braking feeling was the best in this condition. Nevertheless, the scores clearly show that, although there were no false cues, the rumble filter was indeed considered less realistic than the conditions with motion. The score difference between the classical and the one-to-one yaw filters was not large, which was to be expected, since both filters used similar algorithms to cue longitudinal motion. However, for the braking maneuvers, the classical algorithm did not show an improvement with respect to the rumble condition, whereas the one-to-one yaw clearly did. Tentatively, this may be due to the fact that, although both algorithms cued longitudinal motion similarly, they were coupled to different degrees of freedom. The classical algorithm used the central yaw axis and the cabin yaw, whereas the one-to-one yaw used the radius. Moreover, the two filters were dramatically different in the other degrees of freedom, which implies different interactions with the longitudinal motion channel. This cross talk between motion in different degrees of freedom might also be the cause for the small difference between the scores of the two algorithms.

In general, the assessment of new motion drive algorithms is a difficult task, since there is no standard method and it always relies on one specific set of tuned parameters. The comparison with other MDAs rests on the assumption that all motion filters were tuned equally well. In this experiment, we tuned all the motion filters using the authors and a few others as test subjects. The tuning of the classical algorithm was especially difficult. Higher gains, and hence more motion, caused the already mentioned lagging of the roll angle when leaving the curves. Lower gains provided smaller motion cues and it became difficult to distinguish the motion with the classical filter from the motion with the rumble filter. On the whole, the questionnaire method and the breakup of the questionnaire into questions about the longitudinal and lateral motion seems to be a very successful way of understanding the strong and weak points of new concepts for motion cueing.

5.3 Motion Sickness Scales

The main purpose of the experiment was not to investigate motion sickness, so the low scores obtained on the MISC, and the fact that only one subject was unable to finish the experiment, were quite satisfactory. The scores on the MISC were lower with the rumble filter and higher with the classical filter. No statistical difference was found, though, possibly due to the short duration of each run. The higher scores with the classical filter are probably an effect of the false cues present at the end of the curve. The scores at the end of the three runs were on average higher than the scores after the first run, supporting the hypothesis that motion sickness is cumulative.

5.4 Objective Measures

The only relevant metric that showed a significant effect of the motion filter was the maximum deceleration before and at the beginning of the curves and intersections. Maximum deceleration values from real car experiments are not abundant. Brünger-Koch et al. (2006) reported a mean maximum deceleration value of 0.2 g when subjects were asked to make a full stop at a specified point, with an approaching speed of 50 km/hr (~31 mi/hr). Boer et al. (2000) reported mean values between 0.2 g and 0.33 g for approaching speeds between 52 to 65 km/hr (~32–40 mi/hr). Boer et al. also showed results for a 40 m radius, left curve negotiation. With approaching speeds between 72 and 76 km/hr (~45–47 mi/hr), the maximum deceleration values were between 0.23 and 0.36 g (means per subject). Although the experimental settings were different,

the values found in the present study fit well within the ones from tests in a real car.

The mean maximum deceleration values obtained show that in the conditions with motion (classical and one-to-one yaw filters), the maximum deceleration was lower than in the condition without motion (rumble filter). This is in agreement with the findings of Siegler et al. (2001). Siegler et al. performed an experiment on braking behavior in a driving simulator with and without motion. The driving speed was 80 km/hr (50 mi/hr). They reported higher deceleration values in the no motion condition than in the motion condition. For self-initiated braking, the maximum deceleration with the no motion condition was 0.54 g, whereas with the motion condition it was 0.44 g. For braking triggered by sign posts, with the no motion condition, the maximum deceleration was 0.48 g, and with motion, it was 0.43 g. Although these values are larger than the ones obtained in the present study, a few points should be taken into account. First, these values refer to maneuvers where subjects were asked to reach a full stop. Second, the nominal driving speeds were larger than the 50 km/hr (~31 mi/hr) maximum set for the present task. Third, the subjects were asked to reach a full stop at a certain predetermined line. In order to meet the performance goal and decelerate the car to a full stop, the braking maneuver was probably more aggressive than the one needed in the present experiment to approach a curve or intersection. Nevertheless, the higher maximum deceleration with the rumble condition was higher than with the conditions with motion, indicating that for the braking maneuver, motion was indeed relevant.

6 Conclusions

The designed motion drive algorithm showed potential for urban curve driving simulation. The use of the central yaw axis of the Desdemona simulator allows left and right curves with no need to wash out the lateral position. Lateral motion was considered most realistic with the one-to-one yaw filter, although the rumble filter was a very close second. The lower scores of the classical filter, when leaving the curves, were related to the washout of the roll angle at the end of the curve. The results on the lateral motion support the idea that no motion is better than bad motion.

For the longitudinal motion, the no motion condition (rumble) was considered less realistic than the conditions with motion. The only performance metric that was affected by the different motion conditions was the maximum deceleration. Similar to other studies, in the no motion condition, the average maximum deceleration was higher than in the conditions with motion. Comparison with values from real car experiments led us to believe that the addition of motion contributed positively to the realism of the braking maneuver.

Since no specific task or performance goal was set for the experiment, not many behavioral and performance metrics could be used to compare the different filters. The simple task of driving around the city block, keeping in the lane, was not difficult enough to push subjects to their limits. A more demanding task or a very specific performance goal would perhaps force subjects to search for an optimal control behavior. By doing so, the motion cues in the simulator could become crucial in correctly assessing the vehicle state. Further investigation and improvement of the one-to-one yaw motion drive algorithm should include a comparative study between real car driving and simulator driving, setting a clear performance goal and assigning tasks of increased difficulty.

Acknowledgments

The present research was part of the Eureka Project MOVES Σ! 3601. The first author's work was supported by an NWO Toptalent Grant. The authors wish to thank Wytze Hoekstra and Ingmar Stel, for their valuable work on setting up Desdemona for car driving simulation, Paul Bakker, for the extra hours operating the simulator, and Bruno J. Correia Grácio, for helping to prepare and run the experiment.

References

Angeles, J. (2003). *Fundamentals of robotic mechanical systems* (2nd ed.). Berlin: Springer-Verlag.

Berthoz, A., & Droulez, J. (1982). Linear self motion perception. In A. H. Wertheim, W. A. Wagenaar, & H. W. Leibowitz (Eds.), *Tutorials on human motion perception* (pp. 157–199). New York: Plenum Press.

Bertin, R. J. V., Collet, C., Espié, S., & Graf, W. (2005). Objective measurement of simulator sickness and the role of visual-vestibular conflict situations. In *Driving Simulation Conference North America,* 280–293.

Blaauw, G. J. (1982). Driving experience and task demands in simulator and instrumented car: A validation study. *Human Factors, 24* (4), 473–486.

Boer, E. R., Yamamura, T., Kuge, N., & Girshick, A. (2000). Experiencing the same road twice: A driver centered comparison between simulation and reality. In *Driving Simulation Conference Europe,* 69–78.

Brünger-Koch, M., Briest, S., & Vollrath, M. (2006). Virtual driving with different motion characteristics—Braking manoeuvre analysis and validation. In *Driving Simulation Conference Europe,* 69–78.

Burns, D., & Osfield, R. (2004). Open scene graph, A: Introduction, B: Examples and applications. In *Proceedings of IEEE Virtual Reality,* 265.

Chapron, T., & Colinot, J. (2007). The new PSA Peugeot-Citroën advanced driving simulator: Overall design and motion cue algorithm. In *Driving Simulation Conference North America.*

Dagdelen, M., Reymond, G., Kemeny, A., Bordier, M., & Maïki, N. (2004). MPC based motion cueing algorithm: Development and application to the ULTIMATE driving simulator. In *Driving Simulation Conference,* 221–233.

Field, A. (2005). *Discovering statistics using SPSS* (2nd ed.). London: Sage Publications.

Godthelp, H. (1986). Vehicle control during curve driving. *Human Factors, 28,* 211–221.

Godthelp, H., Milgram, P., & Blaauw, G. J. (1984). The development of a time-related measure to describe driving strategy. *Human Factors, 26,* 257–268.

Grant, P. R., Papelis, Y., Schwarz, C., & Clark, A. (2004). Enhancements to the NADS motion drive algorithm for low-speed urban driving. In *Driving Simulation Conference Europe,* 67–77.

Greenberg, J., Artz, B., & Cathey, L. (2003). The effect of lateral motion cues during simulated driving. In *Driving Simulation Conference North America.*

Groen, E. L., & Bles, W. (2004). How to use body tilt for the simulation of linear self motion. *Journal of Vestibular Research, 14,* 375–385.

Hoffman, J. D., Lee, J. D., Brown, T. L., & McGehee, D. V. (2002). Comparison of driver braking responses in a high-fidelity simulator and on a test track. *Journal of the Transportation Research Board, 1803,* 59–65.

Jamson, A. H., Horrobin, A. J., & Auckland, R. A. (2007). Driving: Whatever happened to the LADS? Design, development and preliminary validation of the new University of Leeds driving simulator. In *Driving Simulation Conference North America*. Leeds: University of Leeds.

Jamson, A. H., Whiffin, P. G., & Burchill, P. M. (2007). Driver response to controllable failures of fixed and variable gain steering. *International Journal of Vehicle Design, 45*(3), 361–378.

Kemeny, A., & Panerai, F. (2003). Evaluating perception in driving simulation experiments. *Trends in Cognitive Sciences, 7*(1), 31–37.

Kennedy, R. S., Lane, N. E., Berbaum, K. S., & Lilienthal, M. G. (1993). Simulator sickness questionnaire: An enhanced method for quantifying simulator sickness. *International Journal of Aviation Psychology, 3*(3), 203–220.

Kennedy, R. S., Lilienthal, M. G., Berbaum, K. S., Baltzley, D. R., & McCauley, M. E. (1989). Simulator sickness in U.S. Navy flight simulators. *Aviation, Space, and Environmental Medicine, 60*(1), 10–16.

Nilsson, L. (1993). Behavioral research in an advanced driving simulator—Experiences of the VTI system. In *Proceedings of the Human Factors and Ergonomics Society 37th Annual Meeting,* 612–616.

Panerai, F., Droulez, J., Kelada, J., Kemeny, A., Balligand, E., & Favre, B. (2001). Speed and safety distance control in truck driving: Comparison of simulation and real-world environment. In *Driving Simulation Conference Europe.*

Reid, L. D., & Nahon, M. A. (1985). *Flight simulation motion-base drive algorithms. Part 1: Developing and testing the equations* (Tech. Rep. No. 296). Toronto: University of Toronto Institute for Aerospace Studies (UTIAS).

Reid, L. D., & Nahon, M. A. (1986a). *Flight simulation motion-base drive algorithms. Part 2: Selecting the system parameters* (Tech. Rep. No. 307). Toronto: University of Toronto Institute for Aerospace Studies (UTIAS).

Reid, L. D., & Nahon, M. A. (1986b). *Flight simulation motion-base drive algorithms. Part 3: Pilot evaluations* (Tech. Rep. No. 319). Toronto: University of Toronto Institute for Aerospace Studies (UTIAS).

Repa, B. S., Leucht, P. M., & Wierwille, W. W. (1982). *The effect of simulator motion on driver performance.* (SAE paper

820307.) Warrendale, PA: Society of Automotive Engineers.

Reymond, G., Kemeny, A., Droulez, J., & Berthoz, A. (2001). Role of lateral acceleration in curve driving: Driver model and experiments on a real vehicle and a driving simulator. *Human Factors, 43*(3), 483–495.

Ritchie, M. L., McCoy, W. K., & Welde, W. L. (1968). A study of the relation between forward velocity and lateral acceleration in curves during normal driving. *Human Factors, 10*(3), 255–258.

Schwarz, C., Gates, T., & Papelis, Y. (2003). Motion characteristics of the National Advanced Driving Simulator. In *Driving Simulation Conference North America*.

Siegler, I., Reymond, G., Kemeny, A., & Berthoz, A. (2001). Sensorimotor integration in a driving simulator: Contributions of motion cueing in elementary driving tasks. In *Driving Simulation Conference Europe*.

STSoftware. (2008). StRoadDesign [Computer Software]. Retrieved July 10, 2008, from http://www.stsoftware.nl/StRoadDesign.html.

Toyota News Release. (2007, November 26). *Toyota develops world-class driving simulator. Real-as-possible environment to aid development of active safety technology.* Retrieved on September 15, 2008, from http://www.toyota.co.jp/en/news/07/1126_1.html.

Valente Pais, A. R., Wentink, M., Mulder, M., & van Paassen, M. M. (2007). A study on cueing strategies for curve driving in Desdemona. In *AIAA Modeling and Simulation Technologies Conference and Exhibit*.

Van Winsum, W., & Godthelp, H. (1996). Speed choice and steering behavior in curve driving. *Human Factors, 38*(3), 434–441.

Wentink, M., Bles, W., Hosman, R., & Mayrhofer, M. (2005). Design and evaluation of spherical washout algorithm for Desdemona simulator. In *AIAA Modeling and Simulation Technologies Conference and Exhibit*.

Wertheim, A. H., Ooms, J., de Regt, G. P., & Wientjes, C. J. E. (1992). *Incidence and severeness of seasickness: Validation of a rating scale* (Tech. Rep. No. IZF 1992 A-41). Soesterberg, Netherlands: TNO Institute for Perception.